Angewandte Chemie
Eine Zeitschrift der Gesellschaft Deutscher Chemiker

Supporting Information

69451 Weinheim, Germany

Forming Aromatic Hemispheres on Transition Metal Surfaces

Kwang Taeg Rim,[a,c†] Mohamed Siaj,[a,c†] Shengxiong Xiao,[a,c] Matthew Myers,[a,c] Vincent D. Carpentier,[e] Li Liu,[a,c] Chaochin Su,[a,c,d] Michael L. Steigerwald,[a,c] Mark S. Hybertsen,[b] Peter H. McBreen,[e] George W. Flynn,[a,c] and Colin Nuckolls[a,c*]*

Contributions from:

[a]*Department of Chemistry, Columbia University, New York, NY 10027, USA*

[b] *Center for Functional Nanomaterials, Brookhaven National Laboratory, Upton, NY 11973, USA*

[c] *Center for Electron Transport in Molecular Nanostructures, Columbia University, New York, NY 10027, USA*

[d]*Department of Molecular Science and Engineering, National Taipei University of Technology, Taipei 106, Taiwan*

[e]*Departement de Chimie, Universite Laval, Quebec, QC, G1K 7P4, Canada*

[†]*These authors contributed equally to this work*

(*) Corresponding Authors: George Flynn: phone (212) 854-4162, fax (212) 854-8336, gwf1@columbia.edu and Colin Nuckolls: phone (212) 854-6289, fax (212) 932-1289, cn37@columbia.edu

I. Theoretical Methods:

The DFT calculations for the HBC and Ru-HBC complex were done with Jaguar (versions 5.0, 6.0 and 6.5) [Schrodinger, L.L.C., Portland, OR, 1991-2005.] using a 6-31g** basis for the light atoms and a lacvp** basis for Ru [Wadt, W. R.; Hay, P. J. *Journal of Chemical Physics* **1985,** 82, (1), 284-298.]. Except where specified, complete geometric relaxation was performed. Thermochemistry calculations were performed with hybrid functional of Becke, B3LYP [A. D. Becke, Journal of Chemical Physics **98** (7), 5648 (1993)]. Selected calculations for HBC and the Ru-HBC complexes were done using the generalized gradient approximation (GGA) as formulated by Perdew, Burke and Ernzerhof [Perdew, J. P.; Burke, K.; Ernzerhof, M. *Physical Review Letters* **1996,** 77, (18), 3865-3868]. These lead to the same conclusions concerning structure and orbital distributions described in the text.

II. STM images of a freshly cleaned ruthenium surface.

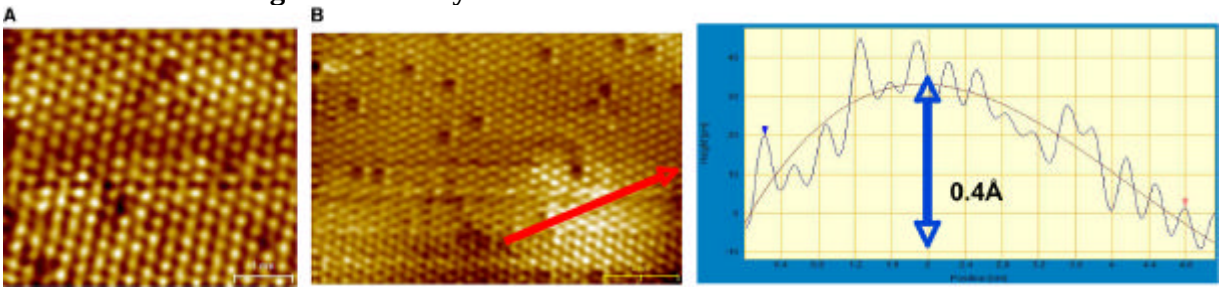

Figure S1. (A) Typical STM topographic image (5 nm x 4.4 nm) of the Ru (0001) surface recorded at room temperature and at *+0.3 V* and *2 nA* shows the hexagonal arrangement of the ruthenium atoms. (B) STM topographic image (9.98 nm x 7.13 nm) of the Ru (0001) surface recorded at room temperature and at *+0.3 V* and *2 nA* shows the underlying features that result from damage during sputtering. The line profile is along the red arrow.

III. Constant current STM image of HBC molecules on Ru taken at negative, positive, and varying bias.

Figure S2 shows the bias dependence of the STM images. At positive tunneling voltages the electron density over the molecular feature is more delocalized than at negative bias. The "bright" hump is also always off-center, however, even at positive tunneling voltages. These images contain information about the frontier orbitals of the adsorbed HBC, in addition to the geometry. The highest occupied and lowest empty orbital of HBC bonded to $Ru(PH_3)_3$ (a proxy for the ad-atom on the surface) are illustrated in Figure S2. The highest occupied orbital in the complex is predominantly a Ru d-state, with weak coupling to the pi states of the pendant phenyl ring. The frontier orbital spatial distribution, taken together with the geometrical distortion, is expected to lead to a sharply asymmetrical STM image at negative sample bias (electron tunneling out of the surface) with the bright spot indicative of the distorted arm and the binding to the Ru. The lowest empty orbital is a more balanced mix of Ru d-states and the pi system on the other arms of the molecule. This delocalization of the empty frontier orbital will tend to render the STM image at positive sample bias (electron tunneling into the surface) more symmetrical.

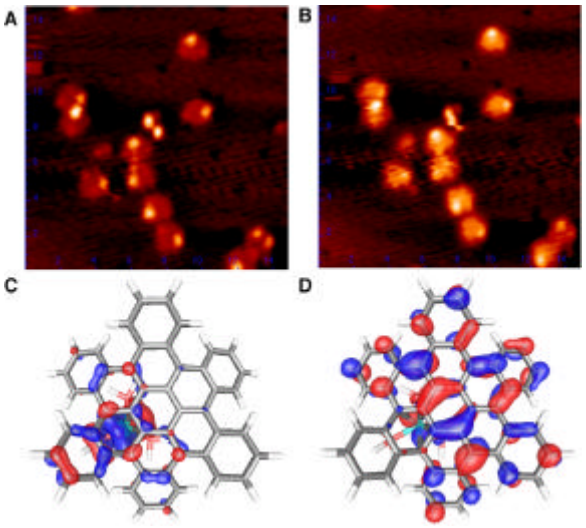

Figure S2. (A) A 15 nm×15 nm constant current STM image of HBC molecules on Ru obtained

at - *0.5 V* and *0.2 nA*. (B) An STM image of the same area as shown in (A), obtained at + *0.5 V* and *0.2 nA*, exhibits the same bright spots in the molecular image as in (A); however the tunneling current over the HBC molecular image appears more delocalized than in (A) taken at negative bias. Isosurface plots of the frontier orbitals from DFT calculations for the HBC•Ru(PH_3)$_3$ system used to model the HBC bonded to an adatom: (C) HOMO; (D) LUMO.

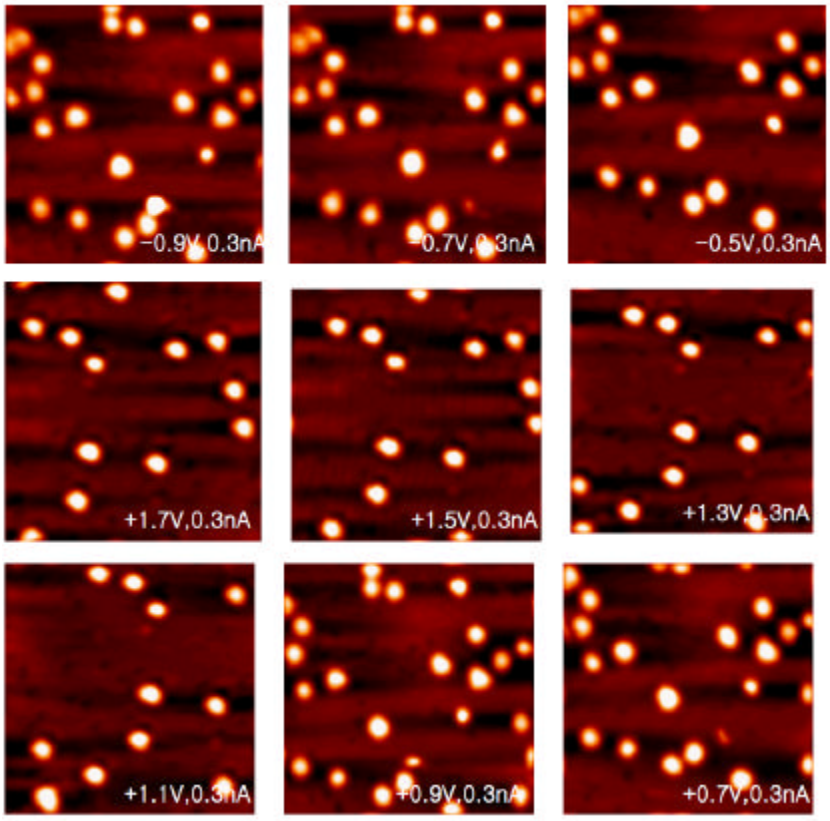

Figure S3. 20nm × 20nm STM images of features after annealing at different bias voltages and different polarities showing no measureable change in the images.

IV. Current-voltage characteristics of the HBC on ruthenium.

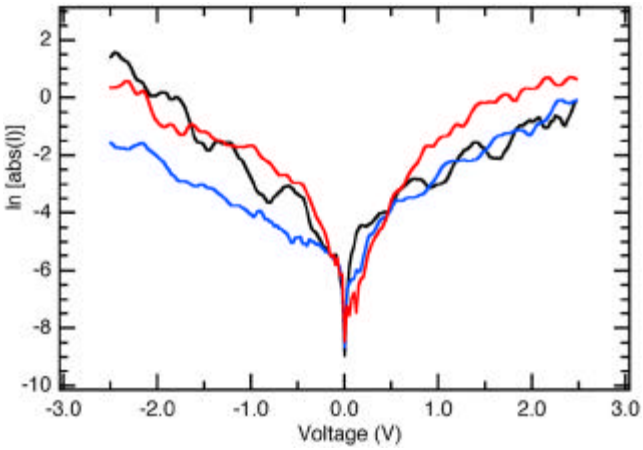

Figure S4. The I(V) curves of bare ruthenium surface (black), after deposition of the HBC

(blue), and after annealing (red).

The black and blue curves were obtained at the scanning conditions of *+1.5V and 0.2 nA*, which set the distance between the tip and molecules/surface, on the bare Ru surface and the HBC, respectively after dosing HBC at the room temperature Ru surface without any thermal treatments. In comparison to the bare ruthenium surface, the initial HBC adsorption causes a substantial reduction in current on the negative bias (electron tunneling out from the surface) side relative to the positive bias (electrons tunneling into the surface) side. These changes suggest strong interaction between the HBC and the Ru surface, displacing state density near the Fermi energy. The red curve was obtained at the scanning conditions of *+1.0V and 0.2 nA* on the HBC after annealing the Ru surface HBC adsorbed on at ~ 600^{o}C. After annealing, this asymmetry is not observed any more. I(V) curve is almost symmetrical between the negative bias side and positive bias side. This suggests that the bonding to the surface is different after annealing.

The changes over the initial HBC site may suggest a chemical interaction between the HBC and the Ru surface, catalytic dehydrogenation of the HBC on the surface forming a bowl-shaped C_{48}. The corrugation of the HBC after annealing, shown in Figure 4C, approximately ~0.2nm, is much larger than ~0.12nm before annealing. Thus, I(V) curve after thermal treatment might exhibit the geometric structure of the annealed HBC, and the electronic structure might have been buried. However, we do not rule out the possibility of electronic structure change of the annealed HBC, shifting the density of states around the Fermi energy and a different chemical interaction with the surface for this species.

V. Reflectance absorbance infrared spectroscopy (RAIRS) and temperature-programmed desorption (TPD)

Vibrational spectroscopy and thermal desorption experiments were performed in a separate ultrahigh-vacuum home made system equipped for reflectance absorbance infrared spectroscopy (RAIRS), temperature-programmed desorption (TPD), and conventional Auger measurements. The base pressure of the chamber was 4×10^{-11} Torr. Reflectance absorbance infrared spectroscopy (RAIRS) was used to measure the vibrational spectrum of the adsorbate exposed surface. Spectra were acquired by referencing 800 sample scans to 800 scans of the clean surface. HBC molecules were introduced into the uhv chamber using organic effusion cell and exposures are expressed as Langmuirs (1 L = 1×10^{-6} Torr s). Narrow band MCT and InSb (not shown) detectors are used to obtain the best signal to noise ratio possible. Desorption spectra were measured by placing the sample face close to the entrance of a shrouded quadrupole mass spectrometer while ramping the sample temperature at a rate of 1 K/s.

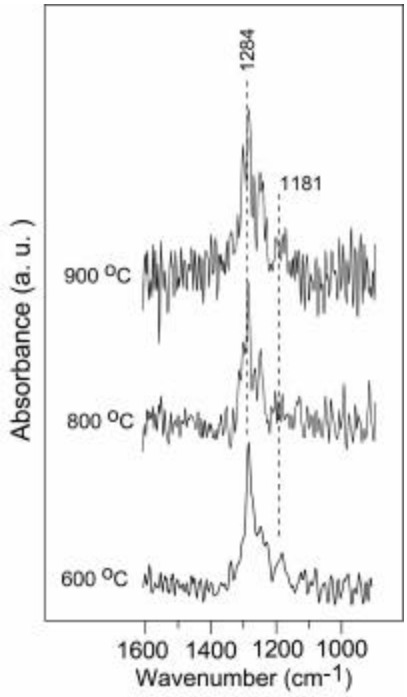

Figure S5. Stability of the hemispherical product after heating to 900 °C.

VI. Structure and thermochemical results for dehydrogenation reactions.

The table below shows the results of DFT simulations of the stepwise dehydrogenation of HBC to give the bowl.

The shorthand of either "ortho", "meta", and "para", or "123", "124", and "135" is used by analogy to di- or tri-substituted benzenes, thus "ortho" means that the two sites that are dehydrogenated to give two five-membered rings are adjacent; "para" means that the sites are on opposite sides of the HBC core, etc.

Included in the table below are total energies (in hartrees) for each calculation. With the equivalent basis set (6-31G**) the total energy for H_2 is –1.178539 h. Comparing these values one can estimate the reaction enthalpies of the stepwise dehydrogenations, and presuming that the lowest-energy isomer is formed at each step, the results are as follows.

HBC	→	HBC(-2H) + H_2	uphill 36 mh (23 kcal/mol)
HBC(-2H)	→	HBC(-4H) + H_2	uphill 35 mh (23 kcal/mol)
HBC(-4H)	→	HBC(-6H) + H_2	uphill 37 mh (23 kcal/mol)
HBC(-6H)	→	HBC(-8H) + H_2	uphill 102 mh (66 kcal/mol)
HBC(-8H)	→	HBC(-10H) + H_2	uphill 88 mh (57 kcal/mol)
HBC(-10H)	→	bowl + H_2	uphill 52 mh (34 kcal/mol)

These calculations use valence double-zeta (6-31G**) basis sets. The numbers may change slightly with larger sets, but not too much. For example, with this double-zeta basis set the enthalpy change from HBC to the bowl + six H_2s is +351 mh; with a larger (triple-zeta) set this goes to +361 mh.

Table S1. Results of DFT simulations of the stepwise dehydrogenation of HBC to give the bowl.

HBC	-1843.705351		
HBC(-2H)	-1842.490502		
HBC(-4H)	ortho	meta	para
	-1841.240029	-1841.277019	-1841.274589
HBC(-6H)	123	124	135
	-1839.993592	-1840.028061	-1840.061180
HBC(-8H)	ortho	meta	para
	-1838.760959	-1838.780853	-1838.771829
HBC(-10H)	-1837.514448		
bowl	-1836.283602		

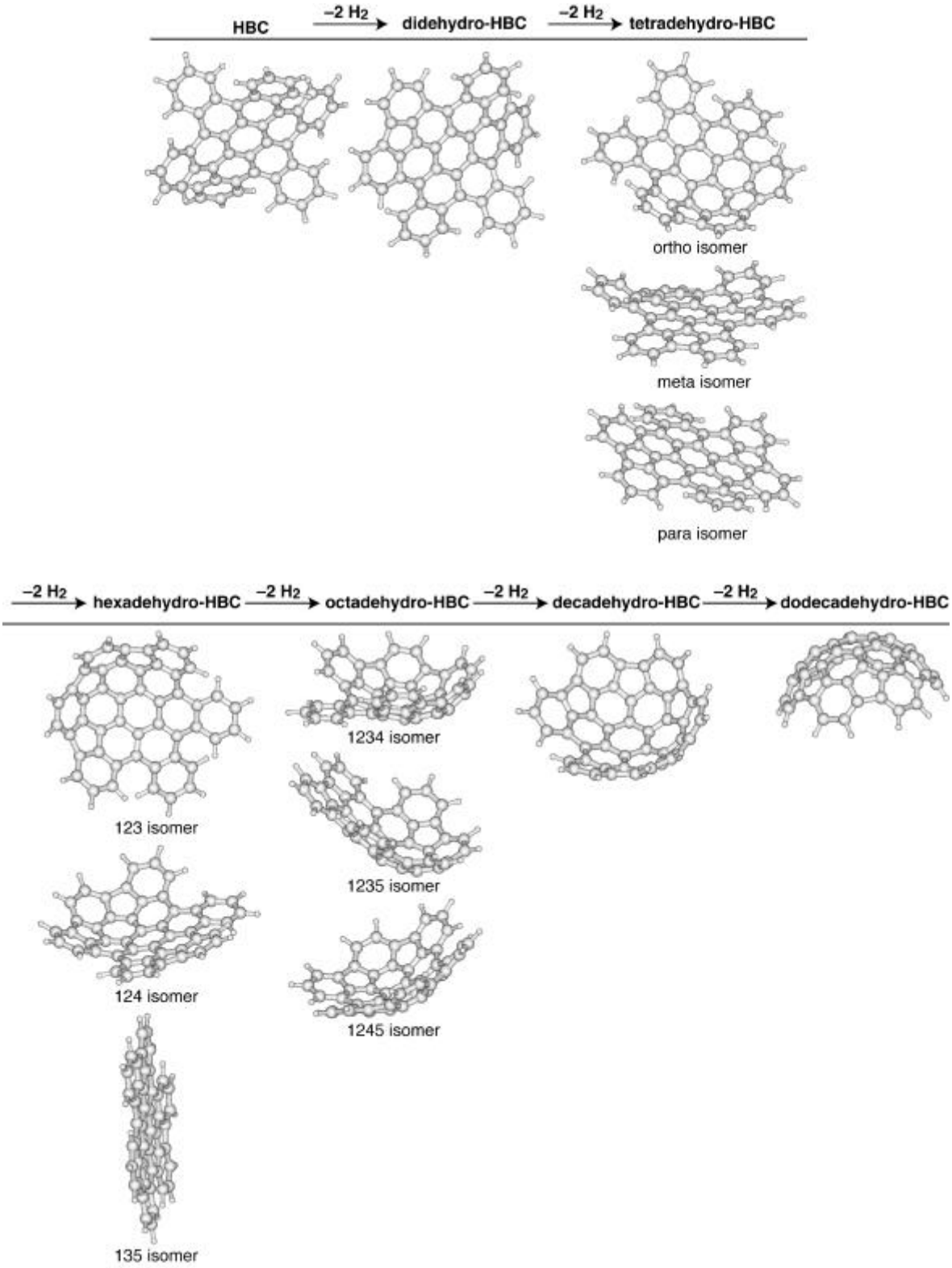

Figure S6. Geometries for each of the successive dehdrogenations from the HBC to the bowl.

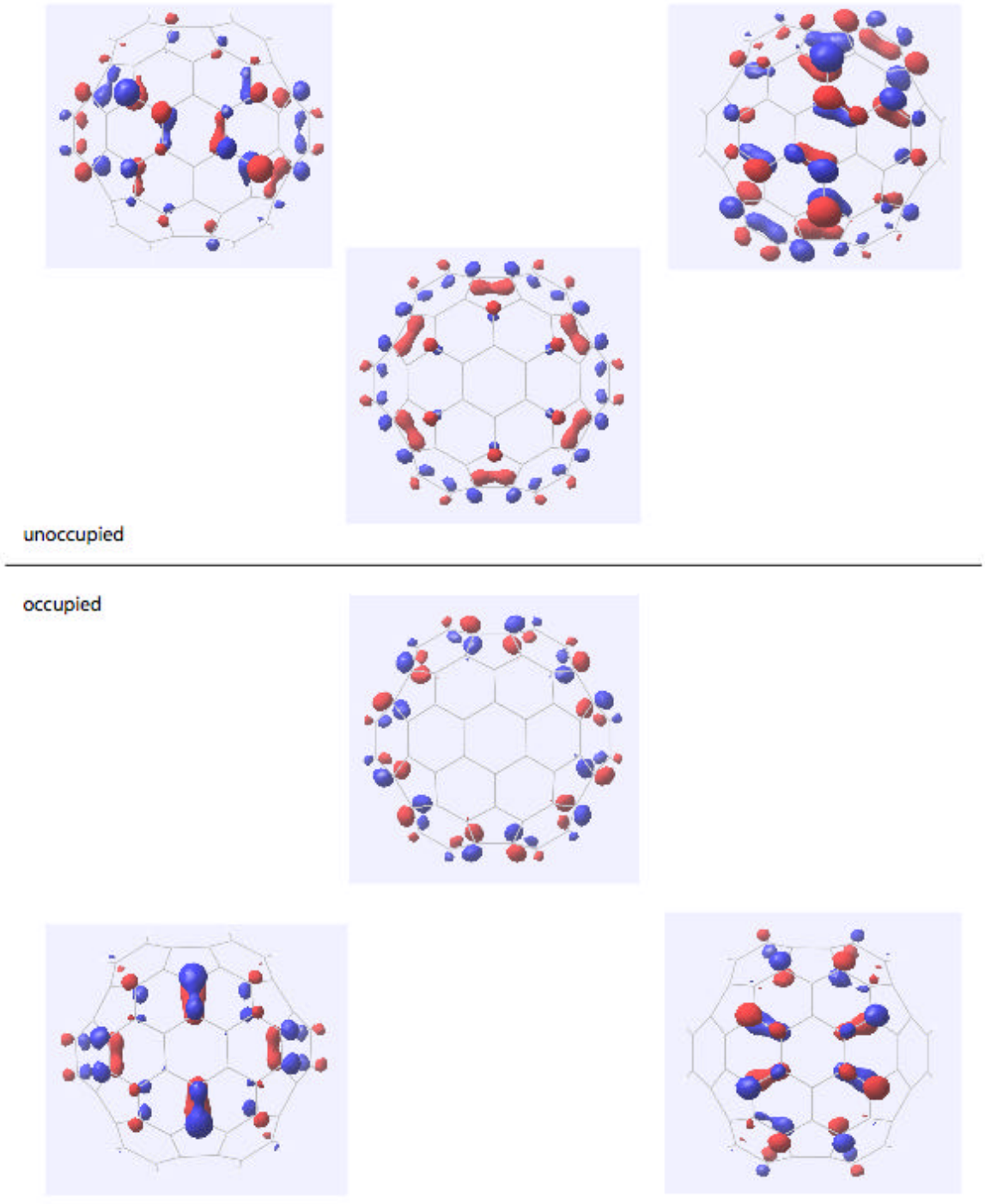

Figure S7. Three highest-energy occupied orbitals and three lowest-energy unoccupied orbitals of the hydrogen-terminated bowl **3**.